

**Cite this article as:** Yang Yanhui, Zhang Zhihong, Chen Xinyi, et al. Reduction in Quenching Residual Stress of 2219 Aluminum Alloy Ring by Cold Bulging Process[J]. Rare Metal Materials and Engineering, 2023, 52(10): 3355-3362.

ARTICLE

# Reduction in Quenching Residual Stress of 2219 Aluminum Alloy Ring by Cold Bulging Process

Yang Yanhui<sup>1,2</sup>, Zhang Zhihong<sup>1,2</sup>, Chen Xinyi<sup>1</sup>, Wang Xin<sup>3</sup>, Zhang Yangyang<sup>1,2</sup>, Liu Yijia<sup>1,2</sup>, Liang Zhengfei<sup>1</sup>

<sup>1</sup> School of Materials Science and Engineering, Northwestern Polytechnical University, Xi'an 710072, China; <sup>2</sup> Chongqing Technology Innovation Center, Northwestern Polytechnical University, Chongqing 400000, China; <sup>3</sup> AVIC The First Aircraft Institute, Xi'an 710089, China

**Abstract:** The mechanical properties of 2219 aluminum alloy can be significantly improved by the solution-aging process. Nevertheless, large residual stress is generated during quenching, exerting negative effects on dimensional stability, fatigue strength, stress corrosion, and other properties. A cold bulging process was introduced between quenching and artificial aging to reduce the quenching residual stress of the 2219 aluminum alloy ring. Firstly, the numerical value and distribution law of the residual stress after quenching and cold bulging of the 2219 aluminum alloy ring were analyzed by finite element method (FEM) simulation. Secondly, the residual stress after quenching, artificial aging and solution-cold bulging-artificial aging of the ring was measured by the drilling method. Additionally, the effect of cold bulging process parameters on residual stress value and uniformity was investigated. Experimental results show that quenching residual stress of 2219 aluminum alloy ring is reduced by up to 85% or more.

**Key words:** 2219 aluminum alloy; residual stress; cold bulging; FEM simulation

Due to high strength at room temperature, good mechanical properties at high and ultra-low temperatures (working in the environment from  $-270$  to  $300$  °C), and excellent stress corrosion cracking resistance, 2219 aluminum alloy is widely used in liquid launch vehicle, space shuttle propellant tank<sup>[1-3]</sup>. Quenching is one of the most vital processes in the heat treatment of high-strength aluminum alloy. Its purpose is to make the second-phase solute completely soluble in the matrix, and then to enable the second-phase elements evenly distributed in the structure through artificial aging, so as to improve the mechanical properties of the metal. However, the temperature difference between the outside and the heart of the workpiece is inconsistent under the existence of a quenching temperature gradient, allowing the material to shrink unevenly and inevitably introducing residual stress. In the subsequent machining process, the release and redistribution of residual stress contribute to the deformation of the workpiece. In the service process, the larger residual stress leads to the initiation of cracks and lowers the fatigue strength of the workpiece<sup>[4-6]</sup>. Therefore, it is of great

significance for the aerospace field to investigate the generation, distribution and control methods of residual stress.

Generally, residual stress reduction method can be divided into three types, namely, heat treatment methods<sup>[7-10]</sup>, electromagnetic methods<sup>[11-14]</sup>, and mechanical methods<sup>[15-17]</sup>. Wu et al<sup>[7]</sup> studied the effect of thermal stress elimination on the reduction and homogenization of residual stress in rolled aluminum alloy rings by finite element simulation and experiment. The results showed that the thermal stress elimination of rolled rings can effectively reduce and homogenize the residual stress. Song et al<sup>[9]</sup> designed a segmental thermal-vibration stress relief (STVSR) device to reduce and to homogenize residual stresses in large 2219 alloy rings with a reduction rate more than 40%. Sun et al<sup>[10]</sup> used a multi-stage interrupted artificial aging treatment to reduce the residual stress of Al-Zn-Mg-Cu alloy thick plates. Pre-deformation is the commonest method to reduce quenching residual stress in mechanical methods, including pre-stretching and pre-compression. Lin et al<sup>[15]</sup> studied the influence of different pre-tensile ratios on the quenching

Received date: December 27, 2022

Foundation item: Chongqing Technology Innovation and Application Development Project

Corresponding author: Yang Yanhui, Ph.D., Associate Professor, School of Materials Science and Engineering, Northwestern Polytechnical University, Xi'an 710072, P. R. China, Tel: 0086-29-88460530, E-mail: yangyh@nwpu.edu.cn

Copyright © 2023, Northwest Institute for Nonferrous Metal Research. Published by Science Press. All rights reserved.

residual stress of Al-Zn-Mg-Cu alloy. Robinson et al<sup>[17]</sup> investigated the effect of cold compression on quenching residual stresses in 7449 aluminum alloy. However, the pre-stretching and pre-compression methods are only applied to workpieces with simple geometries, not ring parts. Some researchers proposed the roll-bending process and mechanical bulging method to regulate the residual stress of rings. Gong et al<sup>[18-19]</sup> proposed a roll-bending method to reduce the quenching residual stress of the large 2219 aluminum alloy ring. The results revealed that the quenching residual stress of the ring decreases after the roll-bending. With the increase in roll-bending times, stress uniformity is improved. At present, the bulging process is primarily employed to control the size of the rolled ring, adjust the roundness, form a special-shaped ring, and enhance the distribution uniformity of residual stress. The principle of bulging is described as follows: under the action of a conical punch, the rigid die moves along the radial direction of the ring and exerts a load on the inner surface of the ring, enabling the radius of the ring to be enlarged<sup>[20-21]</sup>. Wang et al<sup>[22]</sup> found that the cold bulging process reduces the quenching residual stress of 2A14 conical cylinder forgings by 85%. Wei<sup>[23]</sup> and Lv et al<sup>[20,24]</sup> studied the effect of bulging on the rolling residual stress of 2219 aluminum alloy ring and TC4 alloy ring. Simulation and experimental results implied that bulging can improve the uniformity of residual stress after ring rolling. Up to date, fewer works had been reported on the reduction of residual stress in quenched aluminum alloy rings by cold bulging.

In this study, the process of reducing the quenching residual stress of aluminum alloy ring by introducing cold bulging between quenching and aging treatment was proposed. The effect of cold bulging process parameters (bulging ratio and bulging times) on the residual stress of aluminum alloy ring was studied by FEM simulation and experiment, laying a significant foundation for the control of residual stress of 2219 aluminum alloy ring used in aerospace.

## 1 Experiment

### 1.1 Materials

The dimension of the 2219 aluminum alloy rings used in the experiment was  $\Phi 512 \text{ mm} \times \Phi 430 \text{ mm} \times 24 \text{ mm}$ . The chemical compositions of alloy are shown in Table 1.

### 1.2 Experimental procedures

Fig.1 illustrates the processing route of the aluminum alloy ring, and detailed experimental parameters are provided in Table 2. The samples were subjected to solution heat treatment at 535 °C for 2.5 h, followed by quenching in water at 40 °C. Sample E underwent artificial aging, while subsequent treatment was not performed on sample F. Samples A1–D2 were subjected to cold bulging. The cold bulging ratios were

**Table 1 Chemical compositions of the 2219 aluminum alloy (wt%)**

Cu	Mn	Zr	V	Mg	Zn	Fe	Al
5.8–6.8	0.2–0.4	0.1–0.25	0.05–0.25	0.02	0.1	0.3	Bal.

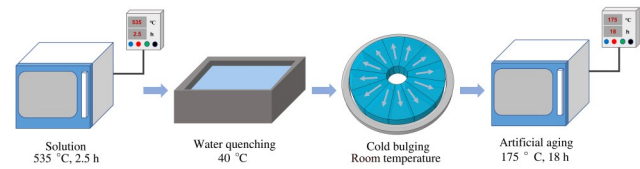


**Fig.1 Schematic diagram of the ring processing route**

**Table 2 Experimental parameters of rings**

Sample	Solution treatment	Water quenching	Cold bulging		Artificial aging
			Ratio/%	Times	
A1	535 °C, 2.5 h	40 °C		2	175 °C, 18 h
A2				3	
B1				3	
C1				2	
C2				3	
D1				2	
D2				3	
E				None	
F	None				

1%, 2%, 3%, and 5% (the inner diameter of the ring was enlarged by 4.3, 8.6, 12.9 and 21.5 mm, respectively), and the cold bulging times were 2 and 3. Subsequently, the samples were aged at 175 °C for 18 h. The time interval between quenching and cold bulging should not exceed 4 h, as well as the time interval between cold bulging and artificial aging, so as to weaken the effect of natural aging on the experimental results.

### 1.3 Evaluation of residual stress

The residual stress on the ring surface was measured by the drilling method. The drilling equipment is a stepper servo-controlled electrical discharge machine, and the strain-gathering equipment is ASMB2-8 type 8-way high-precision static strain detector from Sigma Technology Co., Ltd, Jinan, China, with BE120-2CA-K type strain-gauge rosette. The distribution of measuring points is depicted in Fig.2. The measuring positions are on the end surface and the inner surface, and 8 measuring points were evenly distributed on each surface, with 45° apart. The end surface measurement points are located at the 1/2 wall thickness in the radial direction and the inner surface measurement points are located at 1/2 height of the ring in the axial direction.

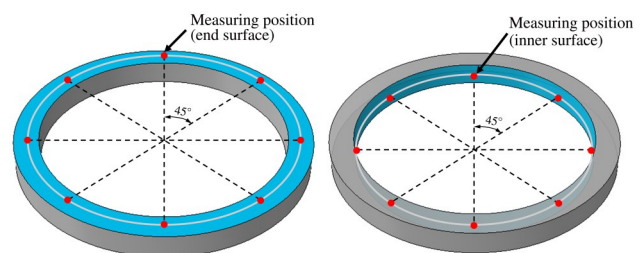


**Fig.2 Residual stress measurement position**

## 2 Simulation

### 2.1 Simulation of quenching

The commercial finite element software ABAQUS was used for the simulation. The material properties of the 2219 aluminum alloy at different temperatures are listed in Table 3. A sequential coupled thermal stress analysis was performed to simulate the temperature and stress fields of the quenching of the 2219 aluminum alloy ring. The temperature field was simulated using the “heat transfer” analysis step with eight-junction linear heat transfer hexahedral elements (DC3D8). Besides, the stress field was simulated through the “static general” analysis step with eight-node linear hexahedral reduction integral elements (C3D8R).

The following assumptions were adopted in the quenching simulation.

(1) The initial temperature field of the ring is uniformly distributed and the initial residual stress in the ring is negligible.

(2) A quench tank of sufficient capacity is used in the quenching experiment to effectively reduce the temperature rise of the quenching medium, which is considered as constant during the simulation.

(3) All surfaces of the ring are in contact with the quenching medium concurrently.

(4) The material of the ring is continuous and isotropic.

(5) The phase change of the ring during the quenching is ignored.

### 2.2 Simulation of cold bulging

The residual stress and geometric model after the quenching simulation were employed as the initial conditions for the cold bulging simulation. Sector dies with 400 mm in outer diameter were used in the simulation, with the same size as the actual experimental dies, and each die has a circular angle of 30°. Fig.3 shows a schematic diagram of the three-

time bulging process. The dies were moved at a uniform speed along the radial direction of the ring, with the dies speed of 1 mm/s. The dies were rotated by 15° after each cold bulging to eliminate the effect of the gap of the dies.

## 3 Results and Discussion

### 3.1 Simulation results of quenching and cold bulging process

The residual stress distribution in different directions after quenching of 2219 aluminum alloy ring is illustrated in Fig.4. It can be observed that quenching induces a large tensile residual stress in the internal region and a large compressive residual stress in the surface region. The distribution range of the Mises stress is 30–160 MPa. The circumferential stress and radial stress of the ring are higher than the axial stress. The circumferential residual stress in the surface region ranges from –134 MPa to –163 MPa, while the radial residual stress ranges from –129 MPa to –177 MPa. The circumferential residual stress in the internal region is between 121 and 178 MPa, while the radial residual stress is between 65 and 114 MPa.

The distribution of stress and strain in rings with different bulging ratios and bulging times is similar, while the values are different. Therefore, only the residual stress distribution with 3% bulging ratio and 3 bulging times was analyzed in this study. Fig. 5 and Fig. 6 present their equivalent strain distribution and residual stress distribution, respectively. Fig.6 demonstrates large strain areas along the circumference of the ring at 30° intervals after cold bulging. This is because there are gaps between each die as the dies are fed radially along the ring during the bulging. Since the ring is not in contact with the die at the gaps, no friction and free deformation occur. Subsequently, the strain at each gap is significantly larger than the area where the two sides are in contact with the dies. From the distribution of the equivalent strain at the cross sections, it can be seen that there is a strain gradient from the inner

Table 3 Material properties of 2219 aluminum alloy at different temperatures

Temperature/°C	25	100	200	300	400	500
Conductivity/W·(m·K) <sup>-1</sup>	159	168	176	180	181	183
Specific heat/J·(kg·K) <sup>-1</sup>	834	838	880	964	1090	1337
Density/kg·m <sup>-3</sup>	2840	2840	2840	2840	2840	2840
Young’s modulus/GPa	71.452	68.346	63.843	58.883	50.880	38.935
Poisson’s ratio	0.33	0.33	0.33	0.33	0.33	0.33
Yield stress/MPa	174.70	–	77.43	44.60	33.11	18.57

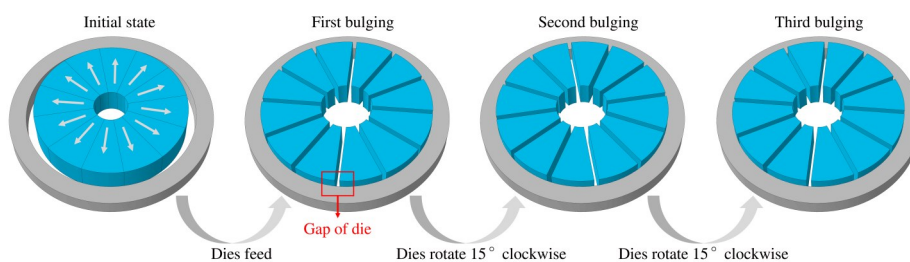


Fig.3 Schematic diagram of three-time bulging process

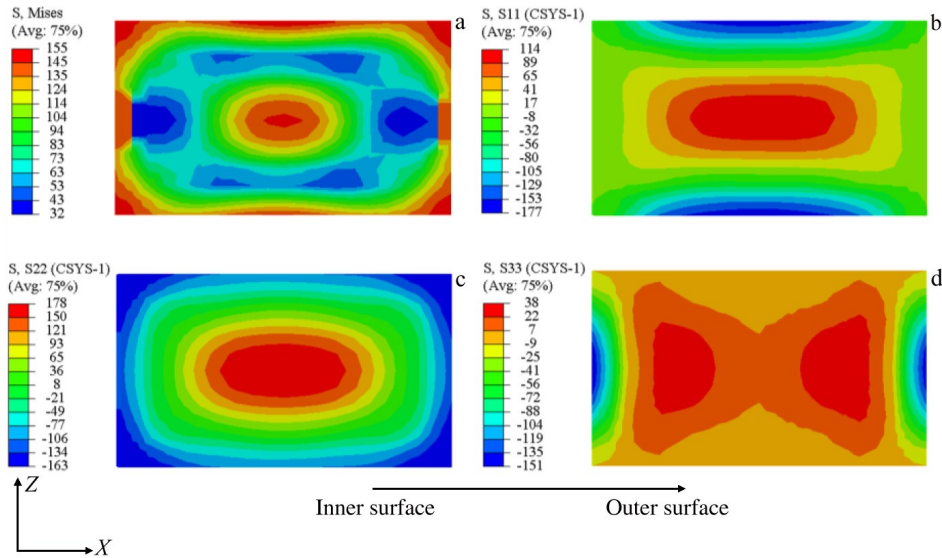


Fig.4 Residual stress distribution in different directions after quenching of 2219 aluminum alloy ring: (a) Mises stress, (b) radial residual stress, (c) circumferential residual stress, and (d) axial residual stress

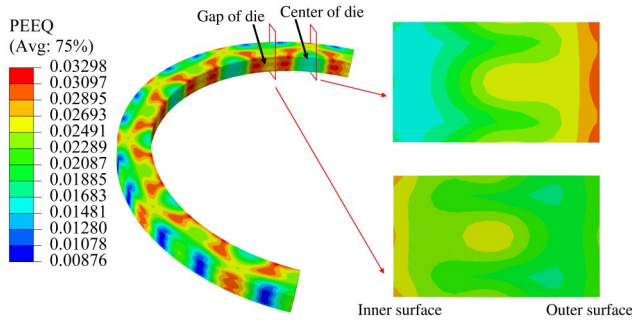


Fig.5 Equivalent plastic strain distribution of 2219 aluminum alloy ring after cold bulging

surface to the outer surface, with a decreasing trend of strain at the gap of die and an increasing trend at the center of the

die. It can be seen from Fig. 6 that the radial stress, circumferential stress, axial stress and Mises stress are all symmetrically distributed along the axial center line of the ring. Similar to the equivalent strain distribution, large stress areas are observed along the circumference of the ring periodically after cold bulging. In addition, the radial, circumferential, and axial stresses of the ring are noticeably reduced after cold bulging.

### 3.2 Experiment results and discussion

Following the actual measuring positions, the residual stress measuring results of 8 points on each measuring surface of the ring are drawn into the residual stress radar map to visually exhibit the residual stress distribution of the ring. Fig. 7 presents the residual stress distribution of 2219 aluminum alloy after quenching (sample F). It reveals a large

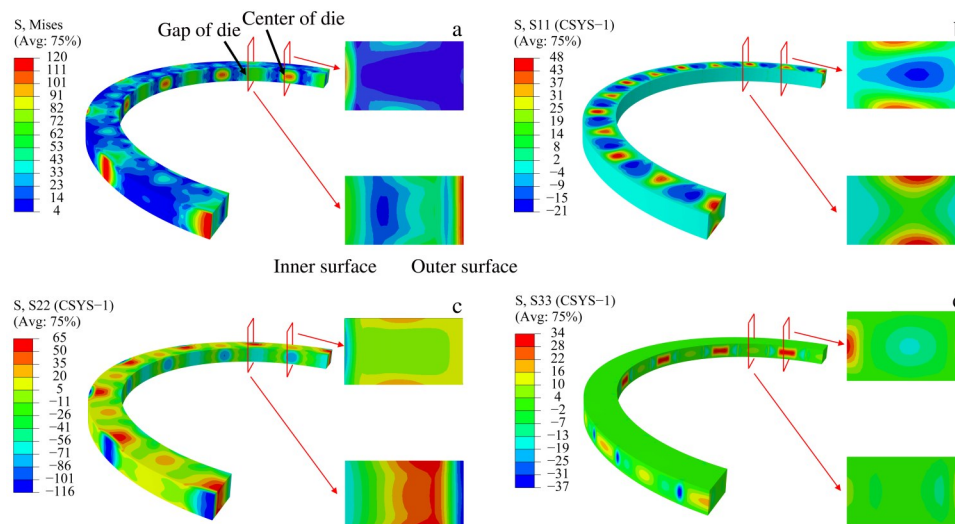


Fig.6 Residual stress distribution of 2219 aluminum alloy ring after cold bulging: (a) Mises stress, (b) radial residual stress, (c) circumferential residual stress, and (d) axial residual stress



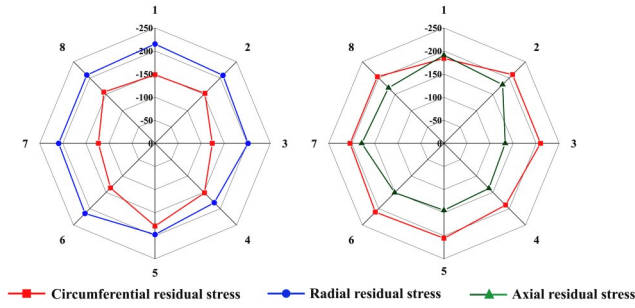


Fig.7 Residual stress distribution of 2219 aluminum alloy ring after quenching: (a) end surface and (b) inner surface

compressive residual stress on the surface of the ring after quenching. On the end surface, the radial stress values are greater than the circumferential stress, with radial residual stress values around  $-200$  MPa and circumferential residual stress values around  $-150$  MPa. On the inner surface, the circumferential residual stress values are larger than the axial stress, with circumferential residual stress values around  $-200$  MPa and axial residual stress values mostly between  $-150$  and  $-175$  MPa.

The residual stress results after artificial aging treatment (Sample E) are shown in Fig.8. Compared with quenching, the residual stress is reduced after artificial aging. The residual stress values on the end surface and the inner surface are nearly equal, around  $-120$  MPa. The change of the residual stress after aging treatment is derived from two aspects. First, the yield strength of aluminum alloy decreases at the aging temperature, and the residual stress exceeding the yield

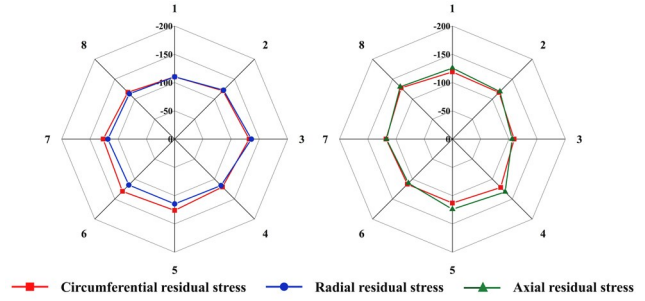


Fig.8 Residual stress distribution of 2219 aluminum alloy ring after solution-artificial aging: (a) end surface and (b) inner surface

strength becomes relaxed due to plastic deformation, which plays a role in reducing the residual stress. Second, the elastic stress field generated by the precipitated phase during the aging process is superimposed with the residual stress field, lessening the residual stress<sup>[25-27]</sup>.

Fig.9 and Fig.10 illuminate the residual stress distribution on the end surface and the inner surface after solution-cold bulging-artificial aging, respectively. Specifically, the quenching residual stress is effectively reduced by introducing a cold bulging process between the solution and artificial aging. Fig.8 shows that the residual stresses in both directions on the same measuring surface after aging are nearly equal, but Fig.9 and Fig.10 show that the circumferential residual stress on the end surface is smaller than the radial residual stress, and the axial residual stress on the inner surface is smaller than the circumferential residual stresses. The main reason for this phenomenon is that the ring is subjected to compressive stress in the radial direction and tensile stress in

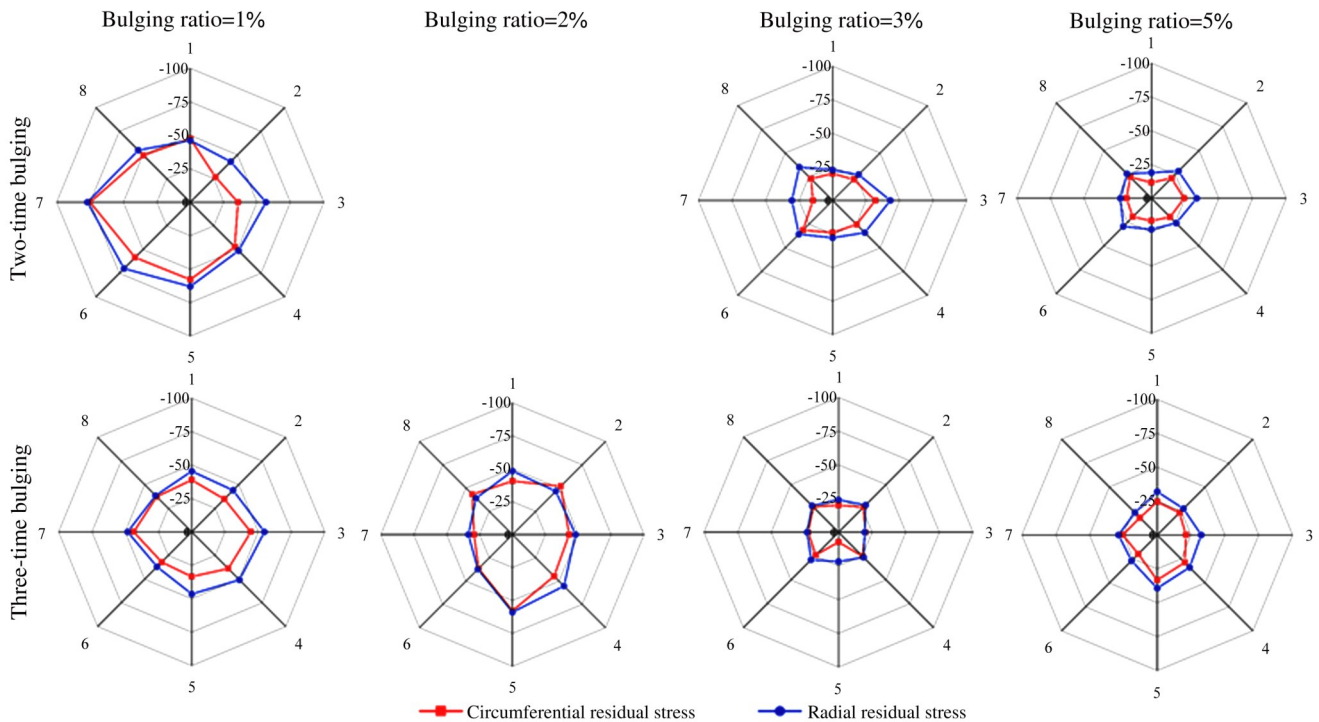


Fig.9 Residual stress distribution on the end surface of 2219 aluminum alloy ring after solid solution, cold bulging and artificial aging

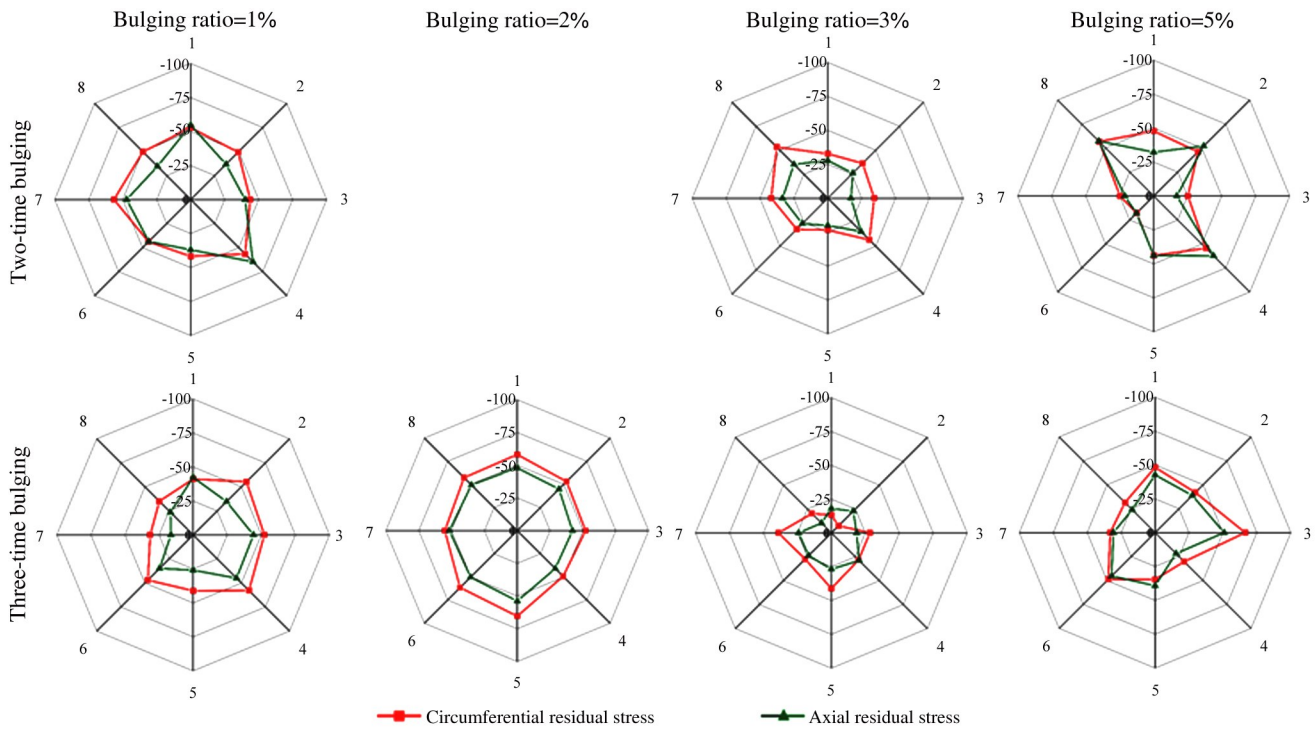


Fig.10 Residual stress distribution on the inner surface of 2219 aluminum alloy ring after solid solution, cold bulging and artificial aging

the circumferential and axial directions during cold bulging, and the circumferential tensile stress is greater than the radial compressive stress. As a result, the reduction effect of cold bulging on the circumferential residual stress of the ring is better than the radial residual stress on the end surface. On the inner surface, the ring undergoes frictional force between the rigid dies and the ring in addition to the bulging force, allowing the reduction effect of axial residual stress on the inner ring surface to be better than that of circumferential residual stress.

Fig. 11 and Fig. 12 illustrate the comparison of average residual stress on the end surface and inner surface of the ring after different processes, respectively. After solid solution and artificial aging, the circumferential and radial residual stresses on the end surface are reduced by 20.0% and 41.7%,

respectively, and the circumferential and axial residual stresses on the inner surface are reduced by 42.0% and 25.0%, respectively. With the introduction of the cold bulging process, the residual stress on the end surface and inner surface is reduced more than 85%. The difference in residual stress between 1% and 2% bulging ratio is not significant. Compared with the cold bulging ratio of 3%, the reduction effect of the residual stress is insignificant when the cold bulging ratio is 5%. The residual stress of three-time bulging is slightly less than the residual stress of two-time bulging (except for the circumferential residual stress on the inner surface) when the bulging ratio does not exceed 3%. The residual stress of three-time bulging is slightly larger than that of two-time bulging (except for the axial residual stress on the inner surface) when the bulging ratio is 5%.

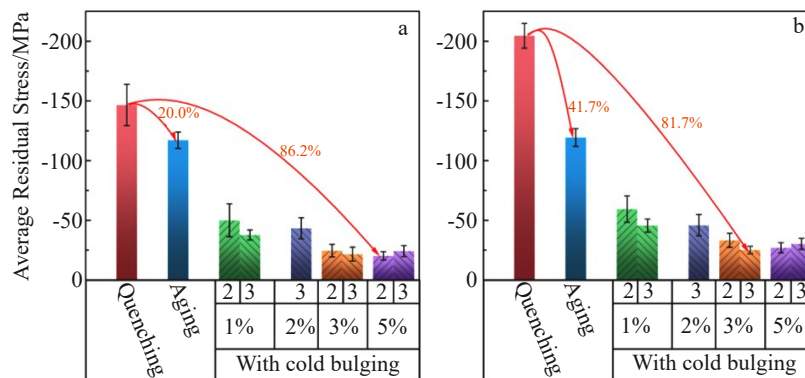


Fig.11 Comparison of average residual stress on the end surface of the ring after different processes: (a) circumferential residual stress and (b) radial residual stress

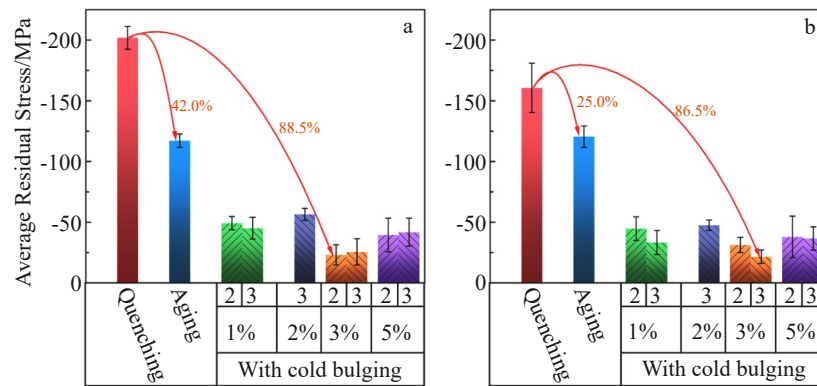


Fig.12 Comparison of average residual stress on the inner surface of the ring after different processes: (a) circumferential residual stress and (b) axial residual stress



Fig.13 “Steps” caused by the cold bulging process

During the cold bulging process, the inner surface of the ring is in contact with the bulging dies and is deformed by the bulging force. Fig. 13 indicates “steps” caused by uneven deformation of the gap part of the dies on the inner surface after cold bulging. The larger the cold bulging ratio, the larger the gap between the dies and the more uneven the deformation, resulting in the deterioration of the uniformity of the residual stress distribution on the inner surface. As suggested in Fig. 10 and Fig. 12, there are acute angle and negative angle positions in the radar map, accompanied by the increased standard deviation of residual stress on the inner surface, when the bulging ratio is 5%.

#### 4 Conclusions

1) The FEM simulation results demonstrate that large residual stress is introduced into the 2219 aluminum alloy ring during quenching process, with tensile stress in the internal region and compressive stress in the surface region. Quenching residual stress is significantly reduced by cold bulging. Due to the gap between the bulging dies, large equivalent strain areas and large residual stress areas are periodically distributed in the circumferential direction.

2) Experimental results reveal that quenching followed by artificial aging can reduce the residual stress by 20%–40%, and introducing cold bulging process between quenching and artificial aging effectively reduces the quenching residual

stress, and the residual stress is reduced by up to 85% or more.

3) The difference in residual stress between 1% and 2% bulging ratio is not significant. Compared with the bulging ratio of 3%, the reduction effect of residual stress is insignificant when the bulging ratio is 5%, and the uniformity of residual stress becomes worse owing to the gap of the dies.

#### References

- Dursun T, Soutis C. *Materials & Design*[J], 2014, 56: 862
- He H, Yi Y, Huang S et al. *Journal of Materials Processing Technology*[J], 2020, 278: 116 506
- Wang G, Zhao Y, Hao Y. *Journal of Materials Science & Technology*[J], 2018, 34(1): 73
- Masoudi S, Amirian G, Saeedi E et al. *Journal of Materials Engineering and Performance*[J], 2015, 24: 3933
- Singh A, Agrawal A. *Journal of Materials Processing Technology*[J], 2015, 225: 195
- Cui J D, Yi Y P, Luo G Y. *Advances in Materials Science and Engineering*[J], 2017, 2017: 1
- Wu Q, Wu J, Zhang Y D et al. *International Journal of Mechanical Sciences*[J], 2019, 157: 111
- Lv N, Liu D, Yang Y et al. *The International Journal of Advanced Manufacturing Technology*[J], 2021, 112(11): 3415
- Song H, Gao H, Wu Q et al. *Journal of Alloys and Compounds*[J], 2021, 886: 161 269
- Sun Y, Jiang F, Zhang H et al. *Materials & Design*[J], 2016, 92: 281
- Li X, Tang Y, Zhang Y et al. *IEEE Transactions on Applied Superconductivity*[J], 2022, 32(6): 1
- Tang F, Lu A L, Mei J F et al. *Journal of Materials Processing Technology*[J], 1998, 74(1–3): 255
- Pan L, He W, Gu B. *Journal of Materials Processing Technology*[J], 2015, 226: 247
- Pan L, He W, Gu B. *Materials Science and Engineering A*[J], 2016, 662: 404
- Lin L, Liu Z, Zhuang W et al. *Materials Characterization*[J],

- 2020, 160: 110 129
- 16 Zhang S, Wu Y, Gong H. *Journal of Materials Processing Technology*[J], 2012, 212(11): 2463
- 17 Robinson J S, Hossain S, Truman C E et al. *Materials Science and Engineering A*[J], 2010, 527(10–11): 2603
- 18 Gong H, Sun X, Liu Y et al. *Materials*[J], 2019, 13(1): 105
- 19 Gong H, Tang H, Zhang T et al. *The International Journal of Advanced Manufacturing Technology*[J], 2022, 119(9): 6863
- 20 Lv N, Liu D, Yang Y et al. *The International Journal of Advanced Manufacturing Technology*[J], 2022, 122(7): 3075
- 21 Lan J, Wei H, Hua L. *Procedia Manufacturing*[J], 2020, 50: 510
- 22 Wang B, Yi Y, Huang S et al. *Metals*[J], 2021, 11(5): 717
- 23 Wei Zhijian, Li Jinshan, Yang Yanhui et al. *Rare Metal Materials and Engineering*[J], 2019, 48(8): 2537 (in Chinese)
- 24 Lv N, Liu D, Hu Y et al. *Engineering Failure Analysis*[J], 2022, 137: 106 269
- 25 Robinson J S, Tanner D A, Van Petegem S et al. *Materials Science and Technology*[J], 2012, 28(4): 420
- 26 Godlewski L A, Su X, Pollock T M et al. *Metallurgical and Materials Transactions A*[J], 2013, 44(10): 4809
- 27 Song Y F, Ding X F, Zhao X J et al. *Journal of Alloys and Compounds*[J], 2017, 718: 298

## 采用冷胀形工艺降低2219铝合金环的淬火残余应力

杨艳慧<sup>1,2</sup>, 张智宏<sup>1,2</sup>, 陈欣怡<sup>1</sup>, 王鑫<sup>3</sup>, 张洋洋<sup>1,2</sup>, 刘宜佳<sup>1,2</sup>, 梁正霏<sup>1</sup>

(1. 西北工业大学 材料学院, 陕西 西安 710072)

(2. 西北工业大学 重庆科创中心, 重庆 400000)

(3. 中国航空工业集团公司航空工业第一飞机设计研究院, 陕西 西安 710089)

**摘要:** 通过固溶时效工艺可以显著提升2219铝合金的力学性能,但在淬火过程中会产生较大的残余应力,对其尺寸稳定性、疲劳强度、应力腐蚀等性能产生不利影响。为降低2219铝合金环件的淬火残余应力,在淬火和人工时效之间引入冷胀形工艺。首先,采用有限元法模拟分析了2219铝合金环淬火、冷胀形后残余应力的数值及分布规律。其次,采用钻孔法测量了环在淬火、人工时效和固溶-冷胀形-人工时效后的残余应力。研究了冷胀形工艺参数对残余应力数值和均匀性的影响。结果表明,引入冷胀形工艺可以使2219铝合金环件淬火残余应力降低85%以上。

**关键词:** 2219铝合金; 残余应力; 冷胀形; 有限元模拟

---

作者简介: 杨艳慧,女,1979年生,博士,副教授,西北工业大学材料学院,陕西 西安 710072,电话:029-88460530,E-mail: yangyh@nwpu.edu.cn